

DESIGN, DEVELOPMENT OF POLYHERBAL NANO FORMULATION- IN SILICO AND IN VITRO STUDIES**M. Vidyavathi^{1,*} T.Srisai Monika² and Dv Sowmya³**

^{1,2}Institute of Pharmaceutical Technology, ³Department of Organic Chemistry, Sri Padmavati Mahila Visvavidyalayam, Tirupati-517502, A.P., India
¹vidyasur@rediffmail.com

ABSTRACT

The active phytochemical constituents of individual plants are insufficient to achieve the desired therapeutic effects. Polyherbalism is a significant therapeutic approach that involves combining many medicinal herbs to enhance their therapeutic effects. Such high effectiveness is due to the presence of different phytoconstituents. Today, Polycystic Ovarian Syndrome (PCOS) is the prevailing female endocrine disorder. Despite the wide variety of medications available on the market, each one of them has its own drawbacks hence, there is a continuous, ongoing research in this area. The present study designed polyherbal nanocrystal formulation by combining powders of *Linum usitatissimum*, *Matricaria chamomilla*, and *Silybum marianum*. Initially, the individual phytoconstituents of the three herbal compounds were evaluated and then docked with PCOS receptors. The *in silico* studies demonstrated that the phytoconstituents (ligands) of three selected herbal compounds have a probability of less GI absorption, along with high protein binding, low V_d , short half-life ($t_{1/2}$), and high (docking scores) affinity with PCOS targets. For the first time, using 3^2 factorial design, the polyherbal nanocrystals (PHNCs) were developed with the selected three herbal combination to improve the bioavailability of herbal compounds by modified single emulsion diffusion method. The optimized formulation with particle size of 306.5 nm, 85.3% entrapment efficiency in elongated crystalline structure and 70% of drug release was developed successfully for treatment of PCOS which was proved by high docking scores

Keywords: *Linum usitatissimum*, *Matricaria chamomilla*, *Silybum marianum*, Polyherbal Nanocrystals, 3^2 factorial, Docking, *In vitro* studies

INTRODUCTION

In recent years, medicinal plants have regained importance due to increased belief in herbal medicine (Sellappan and Ponnambalam, 2014). The recent research has revealed that the combination of herbs enhances the therapeutic effect due to synergism (Kumar et al., 2017).

Linum usitatissimum seeds (Flax seeds) exhibited the presence of lignans and other potent therapeutic compounds and are known in treating PCOS (Debra et al., 2007). *Matricaria chamomilla* also known as Chamomile contains apigenin, α -bisabolol, and other potent therapeutic compounds, which improve the PCOS condition (Zafari et al., 2010). *Silybum marianum*, commonly known as milkthistle, contains three isomeric flavanone lignans, namely silybin (silybin), silychristin, and silydianin collectively called "silymarin" found to be effective in the treatment of PCOS (Kayedpoore et al., 2017). Further the therapeutic efficacy of herbal compounds can be enhanced by development of a nanoformulation (nanocrystals) to increase the absorption of active constituents (Ahmad et al., 2012).

Nowadays, Polycystic Ovarian Syndrome (PCOS) has become one of the most common female endocrine disorders that affects 6-15% of the female population, which is allied with various metabolic disorders (Madhani et al., 2014). This syndrome is one of the main causes of female subfertility, where an imbalance of female sex hormones usually occurs, which leads to elevated androgen levels, menstrual irregularities, and so on. There are a wide variety of medications with hormones and its derivatives available in the market for treatment of PCOS, but those have many side effects. As people nowadays are aware of safety and efficacy of natural remedies, the present study chosen for development of herbal formulations by predicting the activity against PCOS by docking scores in *in silico* studies because molecular docking is a well-known method of molecular

modeling to predict the interaction of a particular ligand with the target receptor protein. The reliability of molecular docking is significantly affected by the accuracy of docking scores and the 3D structure of the receptor (Ajjarapuetal.,2021).

DoE (Designed Experiments or Experimental Design) is a statistical, structured and organized method that has been widely used to support the design, development, and optimization of formulations (Fukuda et al., 2018). so a simple 3² factorial design was applied for optimization of poly herbal nano formulation using two factors at 3 levels.

MATERIALS AND METHODS

LinumUsitatissimum, *Matricaria Chamomilla* powde rand silymarin powders were purchased from Amazon Pvt. Ltd. PLGA, PVA, dichloromethane and other chemicals used in the study were purchased from SD fine chemicals Pvt. Ltd., India.

PHYTO CHEMICAL SCREENING:

LinumUsitatissimum seeds were powdered by using mixer grinder, and passed through sieveno.44 to obtain fine uniform powder. The powders of *L. Usitatissimum*seeds, *M.Chamomilla*, *S.Marianum* were subjected to phytochemical analysis according to conventional methods (Thamilmaraiet al.,2019) for the presence of alkaloids, flavanoids, phenolic compounds, terpenoids, and steroids.

MOLECULAR DOCKING

FDA approved drugs for treatment of PCOS, such as estradiol, spironolactone, clomiphene citrate as control and the ligands from active ingredients of *L. Usitatissimum* seed, *M.Chamomilla*, and *S.Marianum* powders were selected for comparison. The three-dimensional (3D) structures of selected ligands were obtained in simple data format (SDF) from the PubChem server and imported into the UniProt database, where the organism "Homo sapiens" was configured to consistently translate the target's "protein name" into its "gene name" (Duanetal.,2021). The selected ligands of herbal compounds were evaluated for drug likeness and ADME properties. Using Lipinski's rule of five parameters which was derived from the "Molinspiration" tool. Utilizing the ADMET Lab 2.0 software, the toxicity risk was assessed. The corresponding compound SMILES were uploaded into the web server and software in order to accomplish this. The drug likeness to be deemed satisfactory, when it is more than 0.5 (Umaretal.,2021).

The pharmacokinetic properties of the ligands, namely Absorption, Distribution, Metabolism, and Elimination, are crucial in determining their therapeutic efficacy. The rapid, accurate, and user-friendly ADMET Lab 2.0 prediction tool was used to assess ADME attributes for selected herbal constituents(Raj et al.,2021).

PCOS targets were identified and filtered using the terms "polycystic ovarian syndrome" and "polycystic ovary syndrome" in Drug Bank DisGeNET. After then, to prevent duplication, the targets were combined. The selected PCOS target proteins were converted into 3D structures using Schrodinger software with PDB Ids (<http://www.rcsb.org>). The protein-protein interaction analysis was conducted utilizing the String database (<http://string-db.org>) to validate the identification of PCOS targets. Visual analysis findings were produced using Cytoscape 3.7.2. Cluster analysis was conducted using Cytoscape-MCODE, and hub targets were filtered using Cytoscape-hubba (Duanetal.,2021). Then molecular binding affinity was predicted by docking analysis. Protein-ligand docking was performed using pyRx, a virtual screening software for *in silico* drug discovery that allows to screen compounds against a possible therapeutic target (Kambojetal.,2019).

DESIGN OF EXPERIMENT

A two-factor, three-level (3²) factorial design was employed to optimize polyherbal NCs by blending three herbal powders with PLGA and PVA polymers. The independent variables were PLGA content (X1) and homogenization time (X2). These two variables were manipulated across three levels: low (-1), medium (0), and high (+1). The responses or dependent variables examined were particle size (Y1), Entrapment Efficiency (EE%) (Y2), and Poly Dispersity Index (PDI) (Y3).

PREPARATION OF POLYHERBAL NANOCRYSTALS (PHNC)

Total nine poly herbal nano crystals (PHNC1-PHNC9) were prepared (Sharaf et al.,2022) as shown in Table 7. PLGA polymeric nanocrystals containing powders of *L. Usitatissimum* seeds, *M. Chamomilla*, *S. Marianum* were synthesized using a modified single emulsion diffusion process. Initially, PLGA was dissolved in dichloromethane, followed by dissolving the active ingredients (Flaxseeds powder, Chamomile powder, Silymarin) in acetone. The drug and polymer mixture was slowly added to a continuously stirred PVA solution for 10, 15, and 20 minutes, and then sonicated using a probe sonicator. The dispersion was stirred using a magnetic stirrer for 2 hours, then centrifuged at 5000 rpm for 10 minutes and collected the supernatant. The isolated supernatant was then centrifuged again at 9000rpm for 60 minutes, and the resulting nanosuspension was freeze-dried for 48 hours using mannitol (5%w/v in water) as a cryoprotectant to obtain dry nanocrystals.(Shetty PK et al, 2015).

CHARACTERIZATION OF PHNC

Particulate size and PDI:

The particle size (Y1) and Poly Dispersity Index (PDI)(Y3) of prepared polyherbal nanocrystals (PHNCs) were measured using laser dynamic light scattering with a Horiba Zetasizer..

%Entrapment Efficiency (EE %) (Y2):

The %entrapment efficiency (Y2) of PHNCs was determined in triplicate by measuring the quantity of unbound drug in the supernatant using a UV-visible spectrophotometer. The suspension of PHNCs was centrifuged at 12,000 rpm at 4°C for 30 minutes, and the supernatant was then collected. The UV-visible spectrophotometer was used to measure the amount of drug that was not entrapped, and the following formula was used to determine the percentage of drug entrapped in PHNCs: (Sharma et al.,2014).

$$\% \text{Entrapment Efficiency} = \frac{\text{Total amount of drug} - \text{Amount of free drug}}{\text{Total amount of drug}} \times 100$$

STATISTICAL DATA ANALYSIS BY DOE

Development of Polynomial Equations:

The results obtained after evaluation of the 9 formulations for three responses (Y1, Y2, Y3) were fit into different mathematical models as per the design. The model predicted equations were estimated for each dependent variable separately. Polynomial equation includes individual effects, interactive and multiple effects of variables for three responses.

Contour and Response Surface Plots:

For the purpose of diagrammatically representing the influence of variables on the response, contour plots and three-dimensional (3D) response surface graphs were created. They provide support in elucidating the connection between independent factors and responses (Vuddanda et al.,2015).

Optimization of Responses:

Optimization of the selected responses, PS (Y1), %EE (Y2), and PDI (Y3) was carried out by numerical and graphical optimization methods.

The model's reliability was examined by numerical optimization utilizing the desirability approach in order to develop an optimal formulation with desired responses. Graphical optimization was performed by overlaying the critical response onto a contour plot and identifying the feasible response region inside the design space. The optimum values of Y1, Y2, and Y3 were obtained from overlay plots.

Validation of Experimental Design and Optimization:

The responses were evaluated using both experimental methods and the mathematical models developed. The experimental results were compared with the predicted values ramp solutions for quantitative validation of the 3² factorial design.

The %prediction error was calculated using the following equation:

$$\% \text{ Prediction Error} = \frac{\text{Experimental Value} - \text{Predicted Value}}{\text{Predicted Value}} \times 100$$

The composition of optimized formulation was obtained, and was further prepared and characterized by the following studies:

ZETAPOTENTIAL AND SURFACE MORPHOLOGY

The Zetapotential(ZP)for optimized PHNCs (OPHNC) was measured using Horiba Zetasizer. The surface morphology of OPHNC was studied by scanning electron microscope (Philips XL30SEM, Netherlands).The freeze-dried, optimized PHNCs were coated with gold-palladium (Baltec SC030 Sputter Coater, Germany) and were adhered to a piece of double-sided carbon tape that was put on an aluminum stub in order to analyze the surface morphology. (Husseinetal.,2013).

FOURIER TRANSFORM INFRA RED (FTIR)ANALYSIS

FTIR analysis was done to look into how the chemicals used in different herbal formulation and herbal constituents interacted with each other using the Perkin Elmer BX II. The samples were scanned in the IR range from 400to4000cm⁻¹(Sharma etal.,2014).

X-RAY DIFFRACTION (XRD) STUDIES

An X-ray diffractometer with a detector voltage of 40 KV and a current of 30 mA was used to perform X-ray diffraction studies for optimized PHNCs and for the chosen herbal components (flaxseed powder, chamomile powder, and silymarin) using Cu-K radiation. All samples were measured within the 2θ angle range of 5° to 80°, using a stepsize of 0.02 and a scanning rate of 6°/min(Ogunyemietal., 2019).

IN-VITRO DRUG RELEASE STUDIES

The release of silymarin from OPHNCs was assessed using the dialysis bag dissolution technique. The suspension of OPHNCs was placed into a cellulose dialysis membrane with an average width of 25mm. The membrane was immersed in a phosphate buffer of pH 6.4 and tied to the paddle of the dissolution test apparatus. The dissolution process was carried out at a rotation speed of 100 rpm and at a temperature of 37 ±0.5 °C. A 2 ml aliquot was withdrawn from the vessel at specific time intervals (0 min, 15 min, 30 min, 1 hr, 2 hr, 4 hr, 6 hr, 8 hr, 16 hr, and 24 hr)and 2 ml of fresh buffer was added after each withdrawal to maintain the sink conditions. Then the samples were examined using a UV-visible spectrophotometer in order to determine the amount of silymarin released from the membrane into the buffer solution (Sharmaetal.,2014) using its calibration curve developed in buffer by measuring absorbance for concentration range of -visible spectrophotometer (Upendraand Ashish,2013).

HIGH PERFORMANCE THIN LAYER CHROMATOGRAPHY (HPTLC)-FINGER PRINT ANALYSIS

HPTLC fingerprint analysis was used to determine the presence of active components of individual herbs in the OPHNCs. 10 milligrams of individual herbal powder and OPHNCs were dissolved in 10 ml of methanol and then passed through a 0.2mm syringe filter. The obtained filtrate was used for the High Performance Thin Layer Chromatography (HPTLC) analysis. The chromatogram was developed using a mobile phase consisting of toluene, ethylacetate, and formic acid at a ratio of 5:4:1. The Linomat IV automated TLC applicator from CAMAG (Switzerland), the densitometer-CAMAG TLC scanner 3, and the CAMAG CATS 4 software were used

sample was placed in (Track 1: flaxseed powder, Track 2: Chamomile powder, Track 3: Silymarin powder, and Track 4: OPHNCs), and the chromatogram was generated in a 10×10cm twin-trough glass chamber which was saturated with mobile phase. The plates were exposed to the mobile phase for 20 minutes then, allowed to air dry for examination under Ultraviolet light. The chromatograms were analyzed using a densitometer at wavelengths of 254nm, 366nm, and 540nm. The Rf values, peak regions, and fingerprint data were documented using winCATS 1.4.3 software. The Rf values were determined by dividing the solute's distance from the origin by solvent's distance from the origin.

RESULTS AND DISCUSSION

To address the symptoms of PCOS, a combination of Flaxseeds powder (which lowers androgen levels, reduces ovarian volume, and decreases the number of follicles in the ovaries) (Debra et al., 2007), Chamomile powder (which reduces LH/FSH levels, has antispasmodic effects, and prevents premature birth) (Zafariet al., 2010) and Silymarin (which inhibits the proliferation of follicular sheath and reduces testosterone production) (Kayedpoor et al., 2017) was used to produce polyherbal nanocrystals with the purpose of enhancing the bioavailability and therapeutic effectiveness of selected herbal components

Phytochemical Screening:

Phytochemical study is essential for assessing the potential medical uses of plants and to determine the active compounds responsible for their biological effects. The qualitative analysis of phytochemical constituents in flaxseed powder confirmed the presence of phenolic chemicals, terpenoids and steroids. Flavanoids, terpenoids were detected in chamomile powder. The analysis of silymarin revealed the existence of alkaloids, flavonoids, terpenoids, and steroids.

Molecular Docking

For molecular docking studies, 14 ligands were selected for the comparison of the docking scores of selected herbal compounds with the control drugs for PCOS along with their PubChem ID (PCID) are shown in Table 1. These are relevant to Flaxseed powder, Chamomile powder, Silymarin based on the literature, along with control drugs against PCOS targets. Then, the drug likeness, toxicity risk assessment, docking scores, and ADME properties were assessed for the selected ligands. The results of the “drug likeness” of the selected ligands (Table 2) depicted the molecular weight of all the ligands within the permissible range (<500). The number of hydrogen donors of all are in an acceptable range (<10) except Silymarin. The number of hydrogen acceptors (HNA) and the number of atoms were in acceptable limits (<10, <50) respectively. The number of violations of all the ligands is in the range of zero, except for clomiphene citrate. Drug likeness for all the ligands was in the acceptable range (> 0.5). The toxicity risk assessment was measured in terms of Drug Induced Liver Injury (DILI), carcinogenicity, and mutagenicity (Table 3). The toxicity risk assessment values showed that apigenin, silymarin, clomiphene citrate, and spironolactone pose a toxicity risk.

Table. 1: Selected ligands and their PCID

S.No	Herbal compound	Name of the ligand	PCID
1.	Chamomile powder	Alpha bisabolol	10586
2.	Chamomile powder	Alphabisabololoxide B	6432283
3.	Chamomile powder	Apigenin	5280443
4.	Chamomile powder	Caffeic acid	689043
5.	Flaxseed powder	Isolariciresinol	160521
6.	Flaxseed powder	Lariciresinol	332427

7.	Flaxseedpowder	Lignans	443013
8.	Flaxseedpowder	Matairesinol	119205
9.	Flaxseedpowder	p-coumaricacid	637542
10.	Flaxseedpowder	Pinoresinol	73399
11.	Silymarin	Silymarin	5213
12.	Control1	Clomiphene citrate	60974
13.	Control2	Estradiol	5757
14.	Control3	Spironolactone	5833

Table 2: Drug likeness of Selected Ligands

S.No	LigandName	M.Wt (gm/mol)	No. of Hydrogen Donors	No. of Hydrogen Bond Acceptors(HNH)	No.of Violations	No.of atoms	Drug likeness
1.	Alpha bisabolol	222.37	1	1	0	16	0.55
2.	Alpha bisabolol oxide B	238.37	2	1	0	17	0.55
3.	Apigenin	270.24	5	3	0	20	0.55
4.	Caffeic acid	180.16	4	3	0	13	0.56
5.	Isolariciresinol	360.41	6	4	0	26	0.55
6.	Lariciresinol	360.41	6	3	0	26	0.55
7.	Lignans	414.41	8	1	0	30	0.55
8.	Matairesinol	358.39	6	2	0	26	0.55
9.	Pinoresinol	358.39	6	2	0	26	0.85
10.	p-Coumaric acid	164.16	3	2	0	12	0.55
11.	Silymarin	482.44	10	5	0	35	0.55
12.	Clomiphene citrate	405.97	2	0	1	29	0.56
13.	Estradiol	272.39	2	2	0	20	0.55
14.	Spironolactone	416.58	4	0	0	29	0.55

Table 3: Toxicity risk assessment for selected ligands

Name of the Herbal Compound	Ligand Name	DILI	Carcinogenicity	Mutagenicity
Chamomile powder	Alpha bisabolol	---	-	---
	Alphabisabololoxide B	----	-	---
	Apigenin	++	--	-
	Caffeic acid	-	--	--
Flaxseed powder	Isolariciresinol	--	---	--
	Lariciresinol	---	--	--
	Lignans	--	-	---
	Matairesinol	-	-	---
	P-coumaric acid	--	--	---
	Pinoresinol	--	-	--
Silymarin	Silymarin	-	-	--

Control 1	Clomiphencitrate	+++	--	---
Control 2	Estradiol	---	---	---
Control 3	Spiranolactone	-	+	---

Extent of Risk: (---)0-0.1, (--)0.1-0.3, (-)0.3-0.5, (+)0.5-0.7, (++)0.7-0.9, (+++)0.9-1.0

ADME Properties:

All the ligands and the control drugs were screened for Absorption, Distribution, Metabolism, and Excretion (ADME) through the web tool ADMET Lab 2.0. The ADME parameters such as human intestinal absorption (HIA), plasma protein binding (PPB), volume of distribution (Vd), the primary enzyme responsible for metabolism, clearance (CL), and $t_{1/2}$, of the chosen ligands, are provided in Table 4. In the case of absorption, Human Intestinal Absorption (HIA) of all ligands was predicted, and it was found that all of them exhibited poor absorption (>30). The distribution of these compounds was predicted by Plasma Protein Binding (PPB) and Volume of Distribution (Vd). The ligands apigenin from chamomile (97.2%), matairesinol from flax seeds (96.37%), and silymarin (96.65%) had the highest protein binding compared to the controls. This means that the compounds have prolonged action. The volume of distribution (Vd) for all ligands was less than 5 liters, suggesting that the compounds are likely to be limited to distribution in the blood. This is further confirmed by their high protein binding. According to the metabolic prediction, it was found that all the ligands of the three chosen herbal compounds are substrates of CYP2C19 and CYP1A2, just like the control drugs selected for PCOS. There was no significant variance in clearance between the control ligands and plant ligands. The halflife of herbal compounds was short, i.e., <3 hours, similar to the control ligands of PCOS, as shown in Table 4.

Table 4: ADME properties of ligands

Herbal compound	Ligandname	HIA	Distribution		Metabolism	Excretion	
			PPB (%)	VD (L/Kg)		CL ml/min	T1/2hrs
Chamomile powder	Alphabisabolol	>30	94.660	3.378	CYP2C19 Sub (++)	17.911	0.184
	Alphabisabolol oxideB	>30	93.966	1.420	CYP2C19 Sub (++)	11.730	0.287
	Apigenin	>30	97.255	0.510	CYP2C19 Sub (---)	7.022	0.856
	Caffeicacid	>30	87.705	0.370	CYP2C19 sub(+++)	10.973	0.930
Flaxseed powder	Lignans	>30	94.269	1.442	CYP2C19 Sub (+++)	9.551	0.153
	Isolariciresinol	>30	95.666	0.642	CYP1A2 sub(+++) CYP2C19 sub(++)	13.608	0.755
	Lariciresinol	>30	94.126	0.823	CYP1A2sub (+++) CYP2C19 sub(++)	13.371	0.804
	Pinoresinol	>30	94.770	1.052 1	CYP1A2 sub(+++) CYP2C19 sub(++)	7.898	0.435

	Mataresinol	>30	96.378	0.596	CYP1A2 sub(+++) CYP2C19 sub (+)	15.952	0.885
	p-coumaricacid	>30	85.361	0.293	CYP2C9sub 9(+)	6.299	0.919
Silymarin	Silymarin	>30	96.657	0.649	CYP2C9sub (++)	5.144	0.274
Control 1	Estradiol	>30	95.199	1.554	CYP1A2 sub(++) CYP2C19 sub(++)	18.06 4	0.232
Control 2	Spironolactone	>30	91.063	0.672	CYP1A2 sub(+) CYP2C19sub (++)	15.246	0.381
Control 3	Clomiphene citrate	>30	95.430	1.578	CYP1A2 sub (+++) CYP2C19 sub(+)	9.029	0.048

Collection of PCOS targets& Protein Protein Interaction:

The target proteins for all ligands against PCOS are selected through DisGeNET and screened for protein-protein interactions specific to PCOS, as shown in Fig. 1 through the Stringdatabase. The top 10 proteins were selected based on the degree of interaction (Table 5) through Cytoscape, and these proteins were subsequently used for further docking.

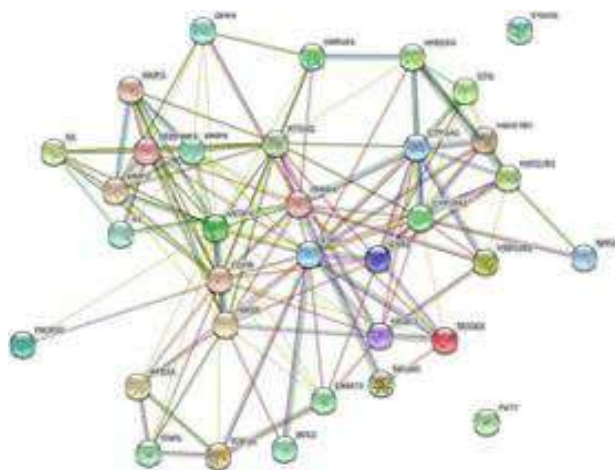


Fig. 1: PCOS Protein interactions with herbal ligands

Table.5: Top ten Proteins selected for docking

S.No	NameoftheProtein	PDBs	Degree
1.	ESR1	1XPC	21
2.	EGFR	4RJ3	20
3.	VEGFA	6ZFL	20
4.	PTGS2	5F1A	16
5.	CYP19A1	3EQM	15

6.	HIF1A	6GMR	15
7.	PPARA	3VI8	14
8.	ESR2	1QKM	13
9.	MMP9	4BAM	13
10.	SERPINE1	4AQH	12

The selected target proteins of PCOS were docked with ligands based on their PDB IDs and visualized in 3D and 2D. The docking scores for each of the target proteins are given in Table 6. The 3D and 2D images of the three target proteins, with the best docking scores (1. 1XPC – 5213: -9.647, 2. 1QKM – 5280443: -9.525, 3. 3VI8 – 443013: -8.707), are shown in Fig.2. The highest docking score was ranged from -10.864 to -2.120. Based on the docking score, the affinity between Silymarin and 1XPC was the greatest among all the interactions whereas apigenin of Chamomile with 1QKM and lignans of Flaxseeds with 3VI8 have shown highest affinity. (Fig. 2). The *insilico* studies showed that the phytoconstituents (ligands) of the three herbal compounds have a probability of less GI absorption with high protein binding, low Vd, less t1/2, high affinity with PCOS targets, and are most likely metabolized by CYP2C19 and CYP21A2.

Table. 6: Docking scores of the target Proteins

S.No	Ligands	PCID	1XPC	4RJ3	6ZFL	5F1A	3EQM	6GMR	3VI8	1QKM	4BAM	4AQH
1	Alpha bisabolol	10586	-6.365	-	-	-5.26	-4.661	-3.951	-	-	-5.219	-3.725
2	Alpha bisabolol oxide-B	6432283	-7.836	-	-	-	-5.417	-5.036	-	-7.508	-6.951	-5.338
3	Apigenin	5280443	-6.437	-	-	-7.25	-5.883	-4.794	-	-9.525	-6.610	-4.902
4	Caffeic acid	689043	-6.462	-	-	-6.26	-5.964	-5.351	-	-7.329	-6.904	-3.997
5	Isolariciresinol	160521	-7.345	-	-	-	-4.980	-6.489	-	-	-6.792	-5.499
6	Lariciresinol	332427	-6.705	-	-	-	-7.874	-5.568	-	-	-7.669	-7.320
7	Lignans	44013	-	-	-	-	-6.188	-3.818	-	-	-7.691	-3.997
8	Matairesinol	119205	-7.515	-	-	-	-8.038	-3.706	-	-6.843	-7.358	-6.277
9	<i>P</i> -coumaricacid	637542	-6.153	-	-	-5.71	-5.827	-5.170	-	-	-6.067	-4.928
10	Piloselinol	73399	-6.489	5.783	-	-	-6.105	-4.341	-	-	-8.814	-7.434
11	Silymarin	5213	-9.647	-	-	-	-7.320	-4.957	-	-	-6.555	-3.731
12	Comphene citrate	60974	-	-	-	-	-7.389	-3.881	-	-	-6.447	-5.007
13	Estradiol	5757	-9.706	-	-	-	-6.969	-4.686	-	-	-6.074	-7.382
14	Spiranolactone	5833	-	-	-	-	-6.701	-	-	-	-5.272	-4.004

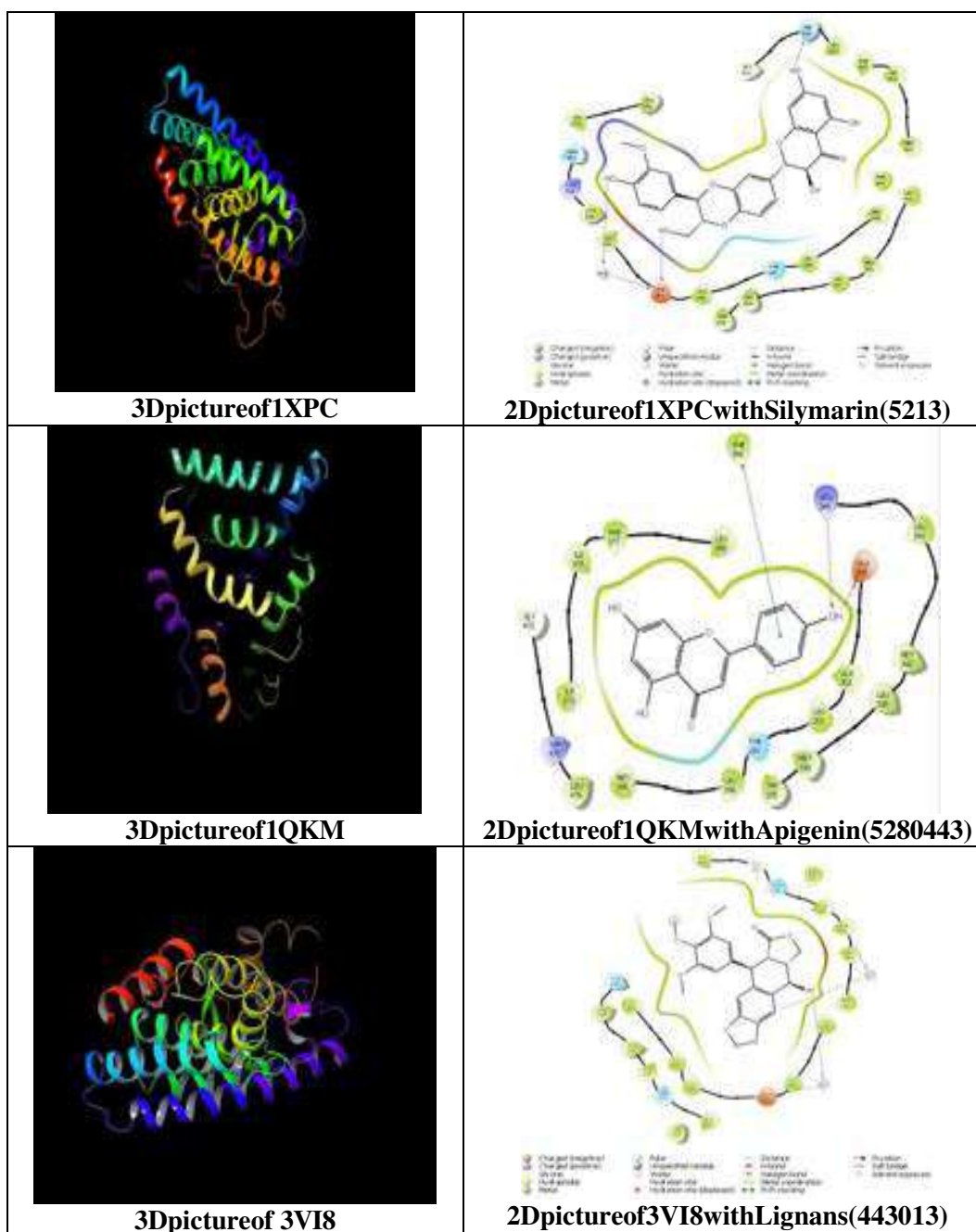


Fig. 2: Binding Mode of Ligands of Best Docking Scores and PCOS (Receptors) Proteins

Characterization of PHNCs

The prepared 9 PHNCs formulations were characterized for Particle size (nm) (Y1), percentage Entrapment Efficiency(%EE) (Y2) and Poly Dispersity Index (PDI) (Y3) and the results are presented in the Table 7.

Table.7: Results of dependent variables (Responses) with coded and actual values of variables

Formulation Code	PLGA		Stirring speed		PS (nm) (Y1)	EE (%) (Y2)	PDI (Y3)
	Coded	Actual (mg)	Coded	Actual (mins)	Mean \pm SD	Mean \pm SD	Mean \pm SD
PHNC1	+1	20	+1	20	237.4 \pm 0.45	82.5 \pm 0.6	0.29 \pm 0.02
PHNC2	0	15	-1	10	230.8 \pm 0.6	77.6 \pm 0.5	0.172 \pm 0.003
PHNC3	-1	10	+1	20	305.6 \pm 0.77	85.3 \pm 0.6	0.525 \pm 0.001
PHNC4	-1	10	0	15	176.5 \pm 0.55	73.4 \pm 0.4	0.413 \pm 0.001
PHNC5	+1	20	-1	10	606.2 \pm 1.1	89.9 \pm 0.8	0.68 \pm 0.015
PHNC6	0	15	+1	20	299.9 \pm 0.97	83.4 \pm 0.7	0.587 \pm 0.002
PHNC7	-1	10	-1	10	209.4 \pm 0.85	77.41 \pm 0.8	0.313 \pm 0.001
PHNC8	+1	20	0	15	314 \pm 1.15	86.5 \pm 0.3	0.279 \pm 0.001
PHNC9	0	15	0	15	113.6 \pm 0.94	67.7 \pm 0.4	0.261 \pm 0.002

ParticleSize(Y1):

The particle size of all PHNC's ranged from 114.5 \pm 0.94nm to 314 \pm 1.15nm (**Table 7**). Contour and response surface 3D plots of particle size and coefficients of the quadratic model are given in **Fig. 3** and equation 1, respectively.

$$Y1 = +156.91 + 60.63X1 - 130.04X2 - 120.66X1X2 + 9.39X1^2 + 244.26X2^2 \dots (1)$$

PLGA concentration (X1) showed a positive relationship with particle size (Y1), indicated that the increase in concentration of PLGA, increased the particle size. This was because PLGA made the organic phase more viscous, which caused bigger nanoparticles to form at the interface (Sharma et al., 2014). In contrast homogenization time (X2) shown a negative relationship with particle size, which indicated the antagonistic effect of X1 on Y2, which may be due to the increased force of deforming droplets at higher speeds, leading to smaller particles (Gupta et al., 2017). But at higher levels, i.e., X1² and X2², they have shown a positive effect. This may be because of the aggregation of particles after optimum PLGA concentration due to decreased surface tension. This is extensively because of the increased erosion effect caused by homogenization, which might induce agglomeration of particles in the liquid by increasing interactions and contact of nanoparticles on the surface of large particles.

%Entrapment Efficiency (Y2):

%Entrapment Efficiency (%EE) of the prepared PHNCs was ranged from 67.7 \pm 0.4 to 89.9 \pm 0.8% (**Table 7**). Contour and response surface plots of entrapment efficiency and coefficients of quadratic model are given in **Fig.3** and equation 2 respectively.

$$Y2 = +71.42 + 4.8X1 - 3.73X2 - 4.86X1X2 + 5.56X1^2 + 13.09X2^2 \dots (2)$$

The concentration of PLGA (X1) exhibited a positive correlation with the %EE, suggesting a synergistic impact. As the concentration of PLGA grew, the percentage of encapsulation efficiency was increased. This is because the diffusion of drug from the organic phase into the aqueous phase is hindered as the viscosity increased at higher levels of X1, which therefore promoted the entrapment (Tefas et al., 2015). The homogenization time (X2) exhibited an inverse correlation with %EE, suggesting an antagonistic impact. Consequently, when the homogenization time increased, the %EE dropped. due to reduction in particle size with homogenization time leads to the leaching of drugs from the nanoparticles (Khatri et al., 2019). The interaction effects of X1X2 exhibit a negative correlation with %EE. However, the multiple impacts of X2² gave a favorable outcome, suggesting that the %EE was increased beyond a specific homogenization duration.

Poly Dispersity Index (Y3):

The Poly Dispersity Index (PDI) of the prepared PHNCs is shown in **Table 7**. The range of PDI was from 0.172 ± 0.003 to 0.68 ± 0.015 . Contour, response surface plots, and the polynomial equation of PDI are shown in **Fig. 3** and equation 3, respectively.

$$Y3 = +0.2774 - 0.053X1 - 0.0537X2 - 0.1401X1X2 + 0.0461X1^2 + 0.2375X2^2 \dots (3)$$

The concentration of PLGA (X1) and the homogenization time (X2) both exhibited a negative correlation with the PDI, suggesting that they have an antagonistic impact on the PDI. An increase in the concentration of PLGA and the homogenization time leads to a decreased poly dispersity index (PDI) indicates that higher levels of PLGA and longer homogenization time would result in the development of much more homogenous NCs (Ismail R *et al*, 2019). The interaction effects of X1 and X2 exhibit a negative correlation with PDI. But, the multiple effects of $X1^2$ & $X2^2$, had a positive result. This suggests that PDI went up when concentration X1 and homogenization time X2 levels were higher than a certain level.

Validation of Model of Responses

The validity of the model was assessed using ANOVA, and the F values obtained for Y1, Y2, and Y3 were 9.62, 9.04, and 0.962, respectively. ANOVA analysis confirmed the model's validity by demonstrating that it was quadratic for all three responses and significant for PS and %EE (F-value = 27.85, $P < 0.0001$). However, the p value for PDI is not statistically significant ($p = 0.548$). The 3D response surface plots along with contour plots further validated the above-stated influence of two factors on the three responses (PS, %EE, and PDI). Further, it was tested by numerical and graphical optimization. The optimized formulation of PHNCs was selected based on a desirability plot with a desirability of 0.817 from the overlay plot in Fig.4.

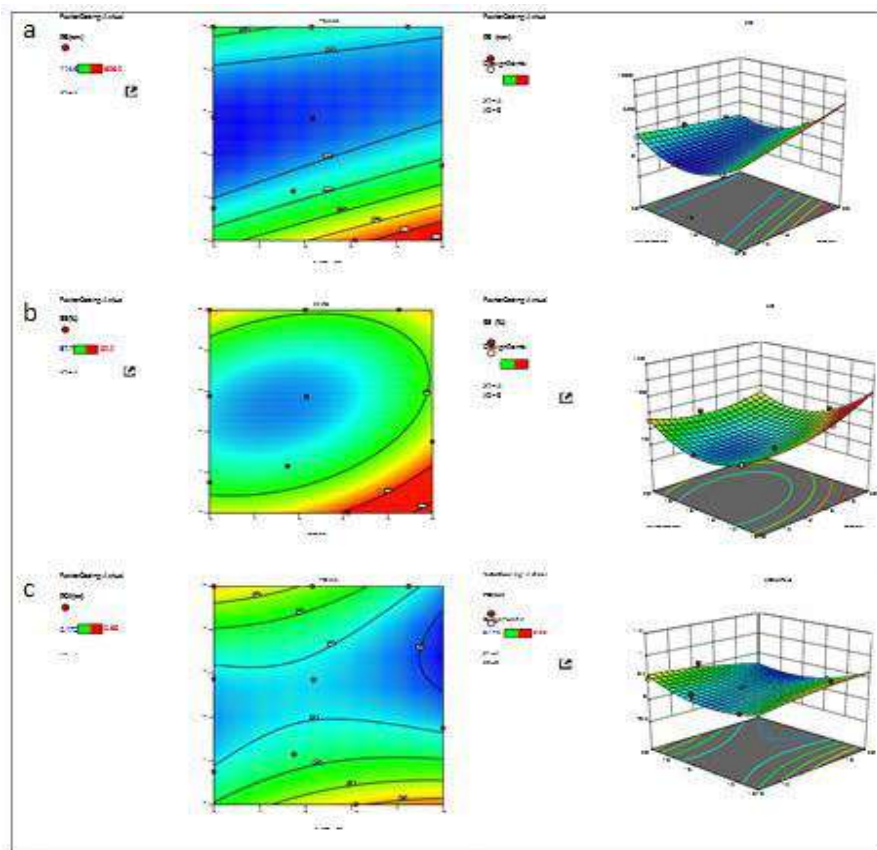


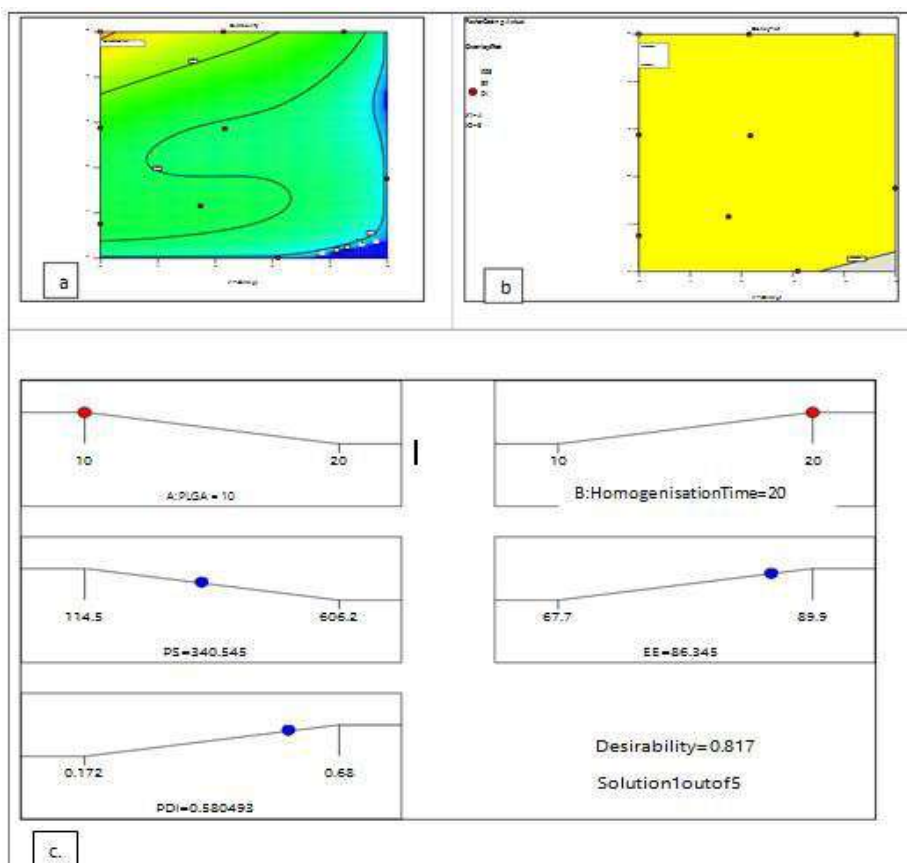
Fig. 3: Contour and 3D response surface plots a) PS (Y1) b) %EE (Y2) c) PDI (Y3)

Optimization of Responses by Numerical and Graphical Optimization:

Further the model was validated by numerical optimization. The overall desirability of the optimized formulation was 0.817. (Fig. 4a). The composition of optimized polyherbal nanocrystals(OPHNC) along with predicted response is obtained from the ramp solution and an overlay plot. Subsequently, the PHNCs were prepared and verified experimentally for three responses and the results were compared with the predicted value. The percentage of prediction error was found to be less than 10%; hence, this model is valid for the development of PHNCs as shown in Table 8. The yellow colored area in overlay plot (Fig .4b,c) was considered as the area fascinating for the desired criteria.

Table. 8: Optimized PHNCS Results

	DoE Predicted value	Experimental value	%Prediction error
Independent variables			
PLGA conc(X1)	10	-	-
Homogenization time (X2)	20	-	-
Dependent variables			
PS (Y1)	340.54	306.2±69.5	10.00
%EE(Y2)	86.345%	85.3%±0.45	1.224
PDI(Y3)	0.580	0.393±0.45	6.77

**Fig. 4:** Optimization By a) Desirability Plot b) Overlay Plot c) Ramps solution for PHNCs

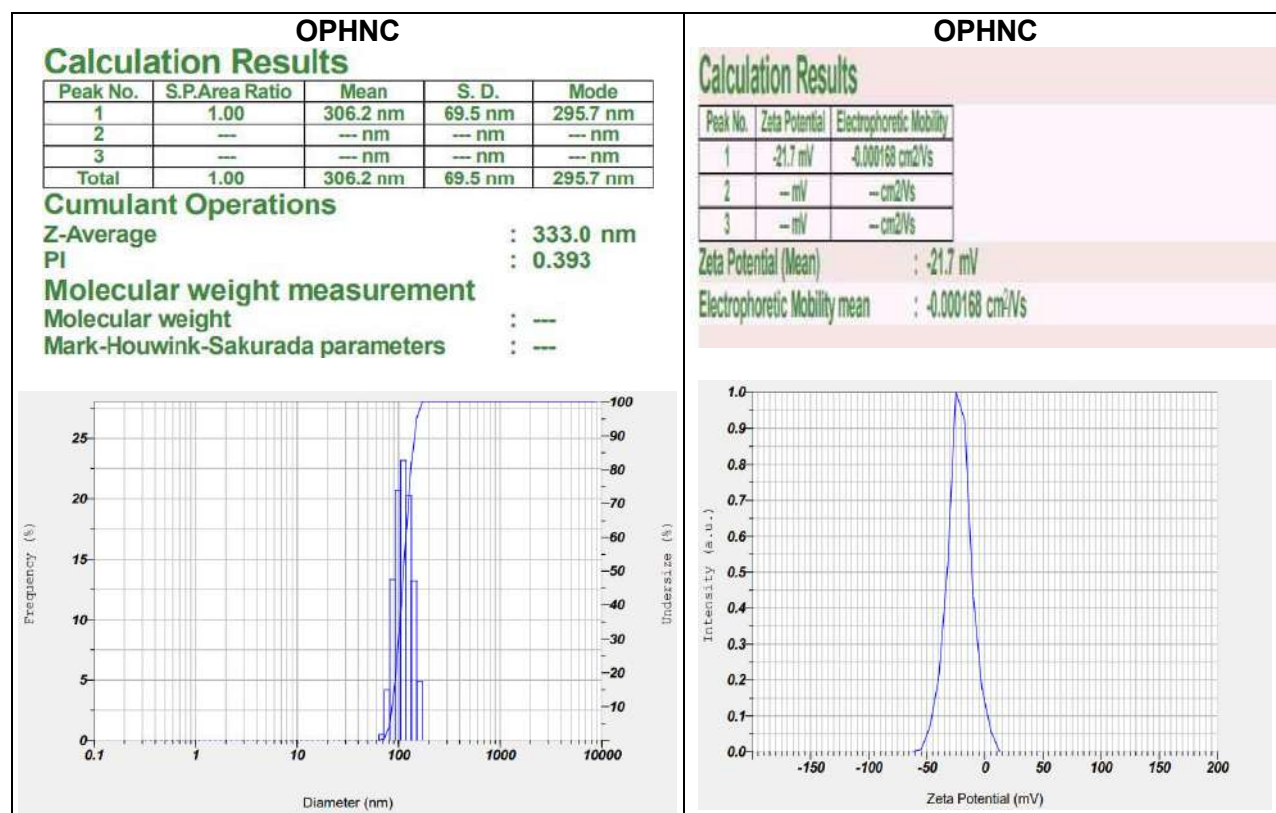


Fig.5: Graphs for particle size and zeta potential of optimized PHNC

Zeta potential and Surface Morphology

Zeta potential of OPHNC was -21.7mV with particle size of 333nm. indicated the stability of OPHNC (Fig. 5). Scanning electron microscopy (SEM) was used to examine the optimized PHNCs. The SEM images (Fig.6) showed that the PHNCs were elongated crystals with irregular shape and crystalline appearance.

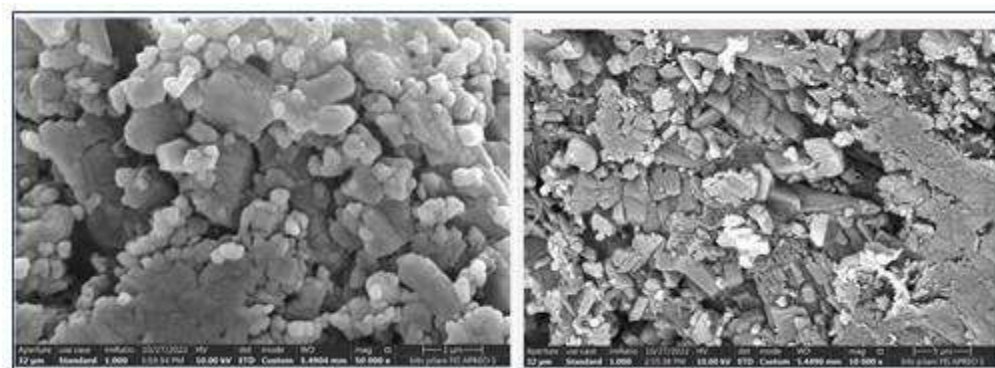
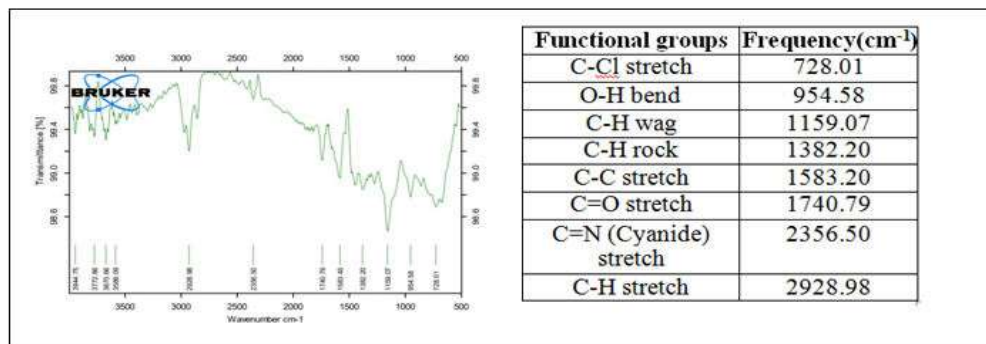


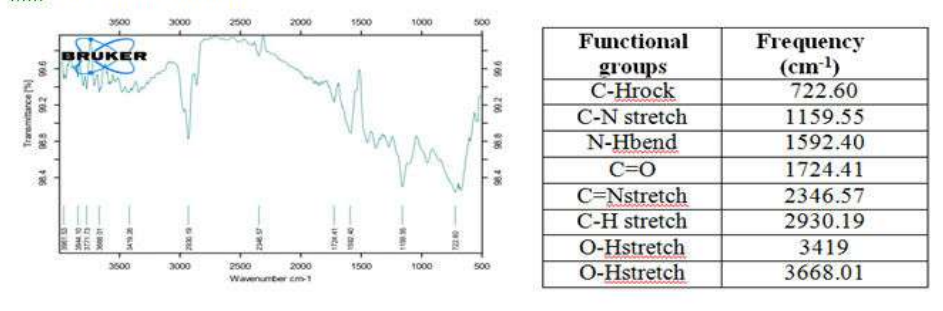
Fig. 6: SEM images of Optimized PHNCs

Fourier Transform Infra-Red (FTIR) Analysis

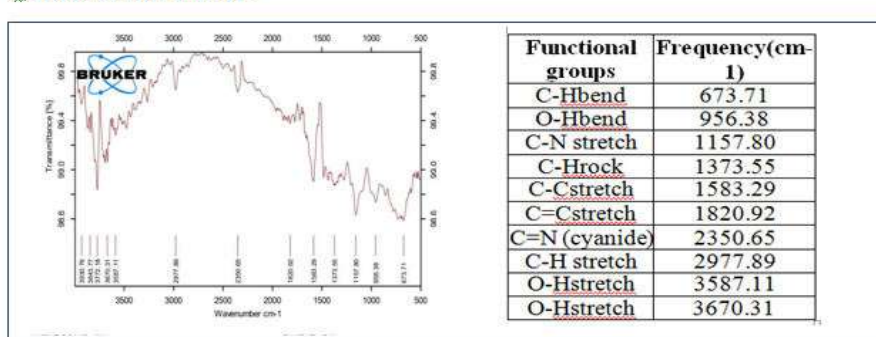
FTIR analysis was performed for Flax seed powder, Chamomile powder, Silymarin and optimized PHNCs at IR range of 400 to 4000 cm^{-1} . The spectra along with the data interpreted, are shown in Fig. 7 that suggested no significant molecular interactions between drug and polymer.



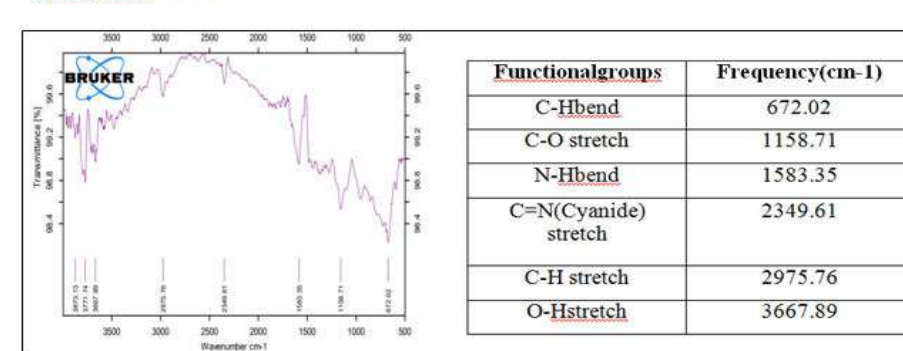
a. : Flax Seed Powder



b: Chamomile Powder



c: Silymarin Powder



d. OPHNC

Fig.7: FTIR spectra & Functional Groups Interpretation of herbal powders and OPHNC

X-Ray Diffraction

The XRD diffractogram of Flaxseed powder, Chamomile powder, Silymarin powder and OPHNCs are shown in Figs. 8 and 9. All herbal powders have not shown any specific sharp peaks, suggesting that they were in an amorphous form. However, the optimized PHNC showed specific sharp peaks at 20° , 24° , 27° , and 36° , indicated that it possessed a crystalline nature.

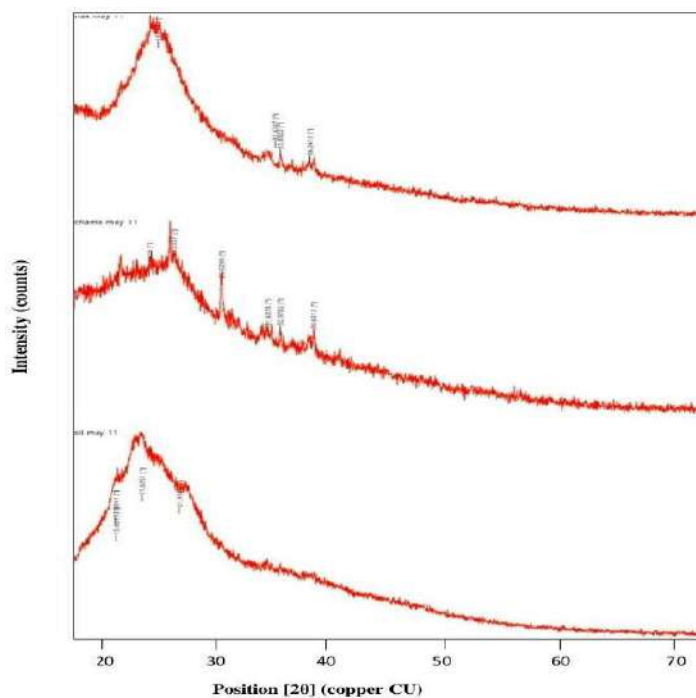


Fig.8: XRD Patterns of a) Flaxseed powder b) Chamomile powder c) Silymarin

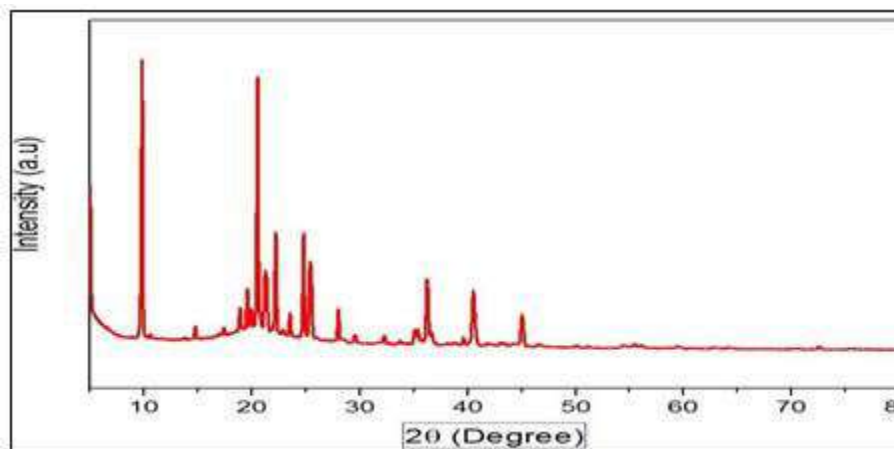


Fig. 9: XRD for Optimized PHNCs

In-Vitro Drug Release Studies of Silymarin:

The % of Silymarin released from OPHNCs was found to be 70.4% in 24 hrs as shown in **Table 9**. The release kinetics was applied to various kinetic models for the dissolution profile of Silymarin from OPHNCs. According to the kinetic results, the release of Silymarin from PHNCs was best fitted into the Higuchi equation (0.939) at a zero-order rate based on the high R^2 values listed in Table 10. This indicated that the drug release from OPHNCs was through the diffusion mechanism.

Table. 9: Silymarin release data from OPHNCs

Time (hrs)	%CDR Mean±SD	log %CDR	Drug remaining	log % drug remaining	log time	square root time	cube root %CDR
0	0	0	0	0	0	0	0
0.25	12.375±0.01	1.093	87.625	1.943	-0.602	0.500	2.313
0.5	25.12±0.02	1.400	87.255	1.941	-0.301	0.707	2.929
1	28.125±0.05	1.449	96.995	1.987	0.000	1.000	3.041
2	34.05±0.06	1.532	94.075	1.973	0.301	1.414	3.241
4	36±0.015	1.556	98.050	1.991	0.602	2.000	3.302
6	44.225±0.016	1.646	91.775	1.963	0.778	2.449	3.536
8	52.6±0.08	1.721	91.625	1.962	0.903	2.828	3.747
16	61.2±0.010	1.787	91.400	1.961	1.204	4.000	3.941
24	70.4±0.0189	1.848	90.800	1.958	1.322	4.583	4.129

Table.10: Drug release kinetic values for model fitting

Kinetic Model	R ² values for OPHNC
Zero order	0.773
First order	0.72
Peppas Model	0.886
Higuchi Model	0.939
Hixson Crowell	0.370

HIGH PERFORMANCE THIN LAYER LIQUID CHROMATOGRAPHY (HPTLC) FINGER PRINT ANALYSIS

HPTLC fingerprint analysis was performed for Flaxseed powder, Chamomile powder, Silymarin powder, and optimized PHNCs at 254nm, 366nm, and 520 nm. 3D fingerprint analysis at 366nm showed good and effective compound separation, as shown in **Fig. 10**, than at 254 and 520nm. The R_f values and peak areas at 366nm are shown in **Table 11 & Fig. 11**. HPTLC fingerprint analysis showed that the R_f values of PHNCs were in close proximity to the R_f values of three herbal compounds (Table 14), with a slight decrease (not significant), which might be due to the loading of herbal compounds into polymeric nanocrystals, leading to the fast elution. Hence, it was confirmed that the OPHNCs contain incorporated herbal compounds.

Table. 11: R_f and peak area values at 366nm

S.No	R _f values				Area(AU)			
	Track-1 (Flaxseed powder)	Track-2 (Chamomile powder)	Track-3 (Silymarin)	Track-4 PHNCs	Track-1 (Flaxseed powder)	Track-2 (Chamomile powder)	Track-3 (Silymarin)	Track-4 PHNCs
1.	0.05	0.05	0.05	0.62	0.00256	0.0008	0.0007	0.0074
2.	0.0655	0.521	0.62	0.82	-	0.0017	0.010	0.019
3.	-	0.636	-	-	-	0.0090	-	-

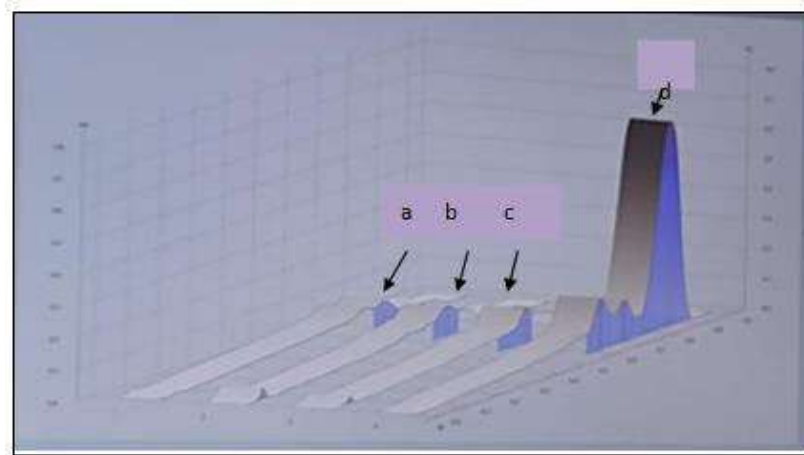
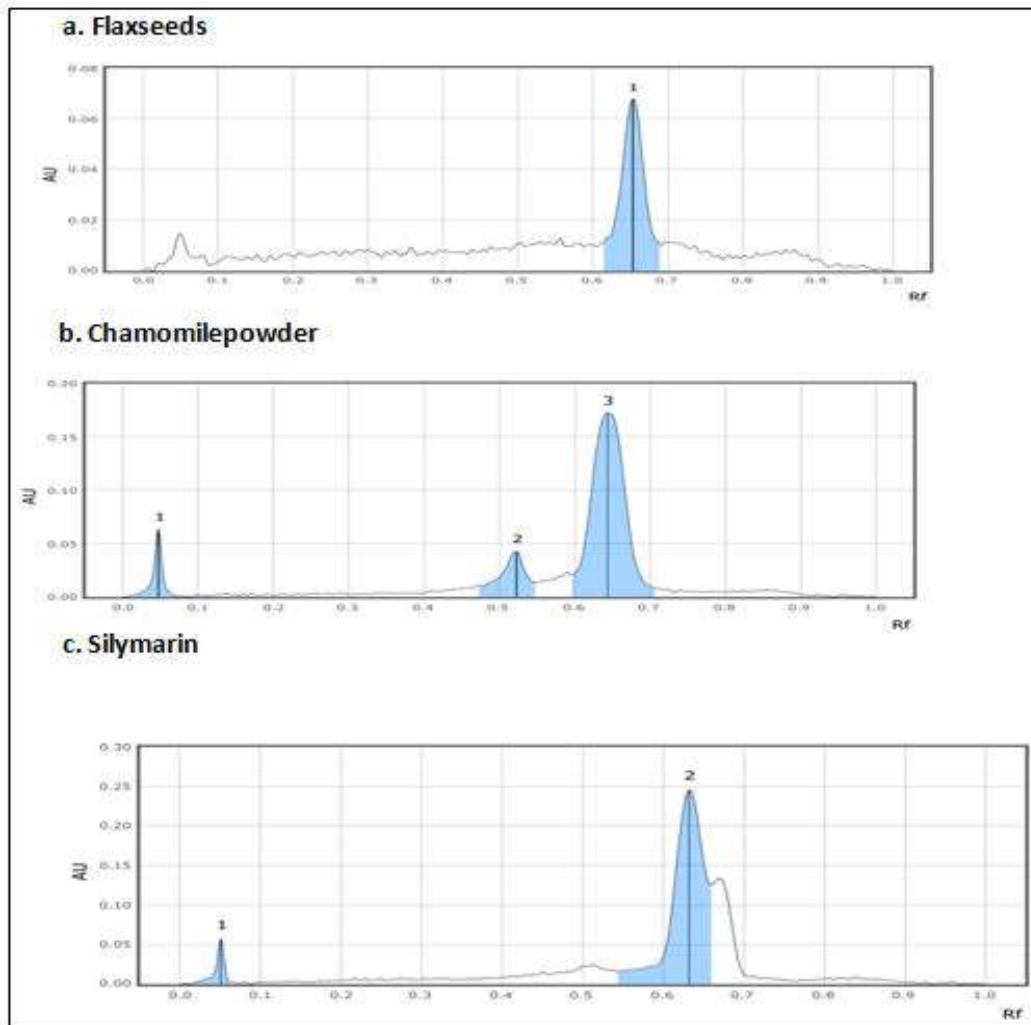


Fig.10: Results of 3D fingerprint analysis of a) Flaxseeds powder b) Chamomile powder c) Silymarin and d)PHNCs



d.Optimized PHNCs

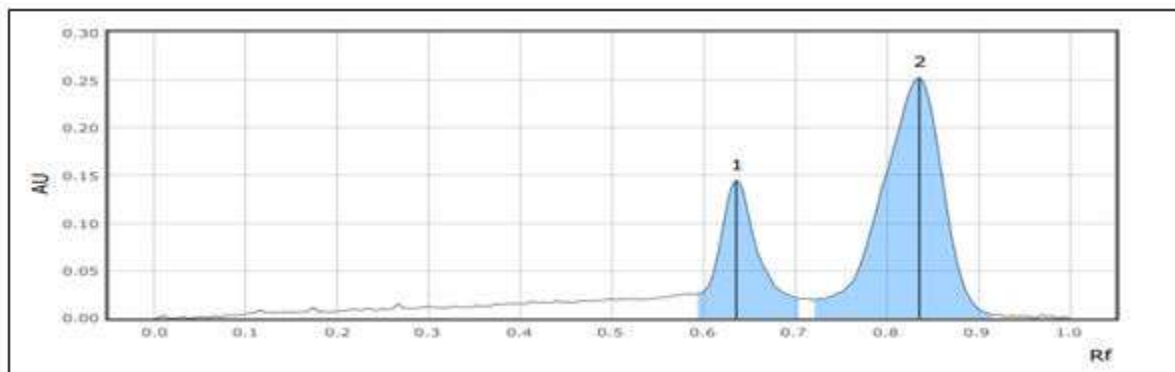


Fig. 11: Rf graphs of HPTLC at 366nm

CONCLUSION

In the present study, poly herbal nanocrystals (PHNCs) of *L. Usitatissimum* powder, *M. Chamomilla* powder, and *S. Marianum* powder was designed, developed to improve the bioavailability of the poly herbal formulation by using a modified single emulsion diffusion technique for the treatment of Poly Cystic Ovarian Syndrome (PCOS) using 3^2 factorial design for the first time. The developed combination of herbal powders may show synergistic action with three different mechanisms to decrease various manifestations of PCOS. The optimized formulation was proved to be valid based on its prediction error. Molecular docking scores revealed that these herbal compounds have good affinity for PCOS targets in *in silico* studies.

ACKNOWLEDGEMENT

The authors are thankful to DST CURIE AI for funding to Sri Padmavati Mahila Visvavidyalayam to conduct Molecular docking studies.

REFERENCES

1. Sellappan.M., and Ponnambalam, H.,2014, "Polyherbal Formulation Development for Anti-Asthmatic Activity," Int. J. of Res. in Pharmacology & Pharmaco therapeutics, 3(2), pp. 90-96.
2. Kumar,S., Dobos,G. J., and Rampp,T., 2017, "The Significanceof Ayurvedic MedicinalPlants," J. Evid. Based Complementary Altern. Med.,22(3), pp. 494-501.
3. Debra, A. N., Denise, C. S., Ann, J. B., and Wendy, D., 2007, "The Effect of Flaxseed Supplementation on Hormonal Levels Associated with Polycystic Ovarian Syndrome: A Case Study," Curr.Top NutraceuticalRes., 5(4), pp. 177-181.
4. Zafari, Z. F., Minaee, B., Amirzargar, A., Ahangarpour, A., and Mousavizadeh, K., 2010, "Effects of Chamomile Extracton Biochemicaland Clinical Parametersina Rat Modelof Polycysticovary Syndrome,"J. Reprod. Infertil., 11(3), pp. 169-174.
5. Kayedpoor,P.,Mohamadi,S.,Karimzadeh-Bardei,L., andNabiuni,M., 2017, "Anti-inflammatoryEffectof Silymarin on Ovarian Immunohistochemical Localization of TNF- α Associated withSystemic Inflammation in Polycystic Ovarian Syndrome," Int. J. Morphol., 35(2), pp. 723-732.
6. Ahmad, M. U., Ali. S. M., and Ahmad, I., 2012, "Applications of Nanotechnology In PharmaceuticalDevelopment," AOCSPress, LipidsinNanotechnology, pp.171-190.
7. Madnani,N., Khan,K., and Chauhan,P., 2014, "PolycysticOvarianSyndrome:A Review," Indian J Dermatol VenereolLeporol., 80(2), pp. 154-155.

8. Fukuda, I. M., Pinto, C. F., Moreira, C. D., Saviano, A. M., and Lourenço, F. R., 2018, "Design of Experiments (DoE) Applied to Pharmaceutical and Analytical Quality by Design (QbD)." *Braz. J. Pharm. Sci.*, pp. 54.
9. Ajjarapu, S.M., Tiwari, A., Taj, G., Singh, D. B., Singh, S., and Kumar, S., 2021, "Simulation Studies, 3D QSAR and Molecular Docking on a Point Mutation of Protein Kinase B with Flavonoids Targeting Ovarian Cancer," *BMCParmacol. Toxicol.*, 22(1), pp. 1-23.
10. Thamilmalai, S.B., Sathammai, P. N., and Steffi, P. F., 2019, "Phytochemical Evaluation, GC-MS Analysis of Phytoactive Compounds, and Antibacterial Activity Studies from *Linum usitatissimum*," *Asian J. Pharm. Clin. Res.*, 12(8), pp. 141-149.
11. Duan, L., Jin, D., An, X., Zhang, Y., Zhao, S., Zhou, R., Duan, Y., Zhang, Y., Liu, X., and Lian, F., 2021, "The Potential Effect of Rhizomacoptidis on Polycystic Ovary Syndrome Based on Network Pharmacology and Molecular Docking," *J. Evid. Based Complementary Altern. Med.*, 2021, Article ID 5577610, pp. 1-12.
12. Umar, H. I., Siraj, B., Ajayi, A., Jimoh, T. O., and Chukwuemeka, P. O., 2021, "Molecular Docking Studies of Some Selected Gallic Acid Derivatives Against Five Non-structural Proteins of Novel Coronavirus," *J. Genet. Eng. & Biotechnol.*, 19(1), pp. 1-4.
13. Raj, D. R., Merlin, N. J., and Dharan, S. S., 2021, "Hinguvachadichoornam, An In Silico Approach to Confirm the Therapeutic Efficacy towards PCOS," *Research J. Pharm. and Tech.*, 14(1), 231-234.
14. Kamboj, A., Verma, D., Sharma, D., Pant, K., Pant, B., and Kumar, V., 2019, "A Molecular Docking Study towards Finding Herbal Treatment against Polycystic Ovary Syndrome (PCOS)," *Int. J. Recent Technol. Eng.*, 8(2S12), pp. 38-41.
15. Upendra, S., and Ashish, B., 2013, "Simultaneous Estimation of Quercetin and Silymarin: Method Development and Validation," *Int. J. Pharm. Biol. Arch.*, 4(3), 527-531.
16. Sharaf, N. S., Shetta, A., Elhalawani, J. E., and Mamdouh, W., 2022, "Applying Box-Behnken Design for Formulation and Optimization of PLGA-Coffee Nanoparticles and Detecting Enhanced Antioxidant and Anticancer Activities," *Polymers*, 14(1), pp. 1-30.
17. Shetty, P. K., Venuvanka, V., Jagani, H. V., Chethan, G. H., Ligade, V. S., Musmade, P. B., Nayak, U. Y., Reddy, M. S., Kalthur, G., Udupa, N., and Rao, C. M., 2015, "Development and Evaluation of Sunscreen Creams Containing Morin-encapsulated Nanoparticles for Enhanced UV Radiation Protection and Antioxidant Activity," *Int. J. Nanomedicine*, 10, pp. 6477-6491.
18. Sharma, D., Maheshwari, D., Philip, G., Rana, R., Bhatia, S., Singh, M., Gabrani, R., Sharma, S. K., Ali, J., Sharma, R. K., and Dang, S., 2014, "Formulation and Optimization of Polymeric Nanoparticles for Intranasal Delivery of Lorazepam using Box-Behnken Design: In vitro and In vivo Evaluation," *Bio Med Res. Int.*, 2014 (156010), pp. 1-14.
19. Vuddanda, P. R., Mishra, A., Singh, S. K., and Singh, S., 2015, "Development of Polymeric Nanoparticles with Highly Entrapped Herbal Hydrophilic Drug using Nanoprecipitation Technique: An Approach of Quality by Design," *Pharm. Dev. Technol.*, 20(5), pp. 579-587.
20. Hussein, A. S., Abdullah, N., and Faku'l-razi, A., 2013, "Optimizing the Process Parameters for Encapsulation of Linamarin into PLGA Nanoparticles using Double Emulsion Solvent Evaporation Technique," *Adv. Poly. Technol.*, 32(S1), pp. E486-504.
21. Ogunyemi, S. O., Abdallah, Y., Zhang, M., Fouad, H., Hong, X., Ibrahim, E., Masum, M. M., Hossain, A., Mo, J., and Li, B., 2019, "Green Synthesis of Zinc Oxide Nanoparticles using Different Plant Extracts and their Antibacterial Activity Against *Xanthomonas oryzae* pv. *oryzae*," *Artif. Cells Nanomed. Biotechnol.*, 47(1), pp. 341-352.

International Journal of Applied Engineering & Technology

22. Gupta,S.,Kesarla,R.,Chotai,N., Misra,A., and Omri,A., 2017, “SystematicApproach fortheFormulation and Optimization of Solid Lipid Nanoparticles of Efavirenz by High PressureHomogenization using Design of Experiments for Brain Targeting and Enhanced Bioavailability,”*BiomedRes. Int.*,2017(5984014), pp. 1-18.
23. Tefas,L. R., Tomuță,I.,Achim,M., and VlaseL., 2015, “Developmentand Otimization of Quercetin-Loaded PLGAN anoparticles by Experimental Design,” *Clujul Med.*, 88(2), 214-223.
24. Khatri, H., Chokshi, N., Rawal, S., and Patel, M. M., 2019, “Fabrication, Characterization and Optimization of Artemether Loaded PE Gylated Solid Lipid Nanoparticles for the Treatment of Lung Cancer,” *Mater. Res., Express*, 6(4), 045014.
25. Ismail, R., Sovány, T., Gácsi, A., Ambrus, R., Katona, G., Imre, N., and Csóka, I., 2019, “Synthesis and Statistical Optimization of Poly(Lactic-Co-GlycolicAcid) Nanoparticles Encapsulating GLP1 Analog designed for oral delivery,”*Pharm. Res.*,36(7), 99.